Nonnegative data interpolation by spherical splines

V. Baramidze [a],[*], M.J. Lai [b]

[a] Department of Mathematics, Western Illinois University, 1 University Circle, Macomb, IL 61455, USA
[b] Department of Mathematics, The University of Georgia, Athens, GA 30602, USA

ABSTRACT

We present a spherical spline method for scattered data interpolation over the unit sphere which preserves nonnegativity of the data values. The method is based on a classic constrained minimization approach. The usual side conditions of smoothness and data interpolation are supplemented by non-negativity constraints. We establish existence and uniqueness of non-negative minimizers in three cases: C^1 spline spaces of odd degree greater than or equal to five over generic triangulations; C^1 cubic spline spaces over Clough–Tocher triangulations; C^1 cubic spline spaces over triangulations of convex quadrangulations. We present the results on approximation order of nonnegative minimizers as well. The method extends to range restricted interpolation. We establish sufficient conditions on the spline coefficients that guarantee range restrictions on the spherical splines. Numerical solutions are computed by means of a projected gradient method. Numerical examples illustrate performance of non-negative and range-restricted data fitting.

© 2018 Elsevier B.V. All rights reserved.

1. Introduction

Spherical splines are piecewise smooth homogeneous polynomials with respect to rectangular coordinates. Given a triangulation $\triangle$ of the unit sphere $\mathbb{S}^2$, a tri-variate homogeneous polynomial can be defined on every triangle in Bernstein–Bézier form. Coefficients of spherical homogeneous Bernstein–Bézier polynomials are found by satisfying side conditions, commonly interpolation and smoothness requirements. Usually, these requirements are not sufficient to find a unique solution, and hence, variational methods are employed. Several minimizing functionals have been successfully used for bivariate as well as spherical splines, for examples see [1–4], and [5]. In this paper, we explore a method for computing a smooth interpolating spline minimizing an energy functional and additionally satisfying range constraints. Shape-preservation of bivariate data has been getting an increasing amount of attention in recent years [6–23]. Many applied problems require fitting surfaces to have additional properties such that convexity, monotonicity and/or nonnegativity. For example, the researchers in [22] proposed a method for computing nonnegative splines, and used it to find an interpolant for deep water oxygen deficit values [24] over a polluted region in the Gulf of Mexico.

Non-negativity of a spherical function, $f(x, y, z) \geq 0$, is perhaps the most straight forward concept of shape-preservation on a plane that can be directly translated into the spherical setting. Some phenomena are range restricted by nature. For example amount of rain, absolute temperature, or specific humidity are all non-negative values, and are often of interest in natural sciences. In our numerical experiments we present an example of a nonnegative spline interpolating specific humidity data collected around the globe. See Fig. 9 and numerical results in Section 5.

---

* Corresponding author.
   E-mail addresses: V-Baramidze@wiu.edu (V. Baramidze), mjlai@math.uga.edu (M.J. Lai).

In general, given a set of data $\{(v_i, f_i) : v_i \in \mathbb{S}^2, f_i \geq 0, i = 1, \ldots, N\}$, with f_i viewed as a value of some smooth function f at the location on the sphere v_i, we wish to construct a spline $S(v)$ which

- interpolates the data, i.e. $S(v_i) = f_i, i = 1, \ldots, N$;
- has a desirable smoothness, i.e. $S \in C^r(\mathbb{S}^2), r \geq 0$;
- is nonnegative, i.e. $S(v) \geq 0, \forall v \in \mathbb{S}^2$, or, if the data values f_i vary within a range $[a, b]$, then the values of S should be within the same range;
- improves its approximation of f as the number of available data increases while sustaining uniform coverage of the domain.

Note that the last item on the list, i.e. the data fidelity, is the most important requirement in the data fitting problem. See [25] and [26] for spherical spline convergence studies for fitting problems without shape-preservation. Approximation results for nonnegative spherical splines produced by the proposed method are presented in Section 3.

There are many studies on nonnegative/range-restricted interpolating schemes, for examples see [6,10,12,16,19,21,27–31] and references therein. In [22] the researchers proposed a global constrained minimization approach for computing nonnegative interpolating splines. The authors showed that when the interior edges of the given triangulation Δ are active, the feasible set in $S_5^1(\Delta)$ is nonempty and hence the constrained minimization problem has a unique solution. The projected gradient method was used to compute the minimizer, and it was proved that the minimizer converges to the sampled function f if $f \in C^2$. In this paper we extend the study to the spherical setting. Let us point out some key differences between this study and the results presented in [22]. First of all, we introduce a concept of a quasi-active triangulation refinement. The refinement allows us to drop an active edge requirement while keeping the space of splines, and the feasible set in it, big enough to guarantee the existence of a nonnegative solution. Furthermore, we show how to construct the nonnegative splines in cubic C^1 spline spaces over Clough–Tocher refinements and quadrangulations, as well as odd degree spline spaces with $d \geq 5$ over quasi-active refinements of generic triangulations. At last, we present sufficient conditions on the coefficients of range-restricted splines which are different from those in the planar setting.

Allow us to review some relevant information on spherical splines. Let Δ be a triangulation of the unit sphere $\mathbb{S}^2$. For two positive integers $r \geq 0$ and $d > r$,

$$S_d^r(\Delta) := \{s \in C^r(\mathbb{S}^2) : s|_t \in \mathbb{H}_d, \forall t \in \Delta\}$$

is the space of homogeneous spherical splines of smoothness r and degree d over triangulation Δ (cf. [32]), where $\mathbb{H}_d$ is the space of all homogeneous polynomials of degree d on $\mathbb{S}^2$, and t is a spherical triangle in Δ. Piecewise polynomial functions over a triangulation are very efficient for computation and hence are excellent for numerical approximation. It is known that $S_d^r(\Delta)$ with $r \geq 1$ can be used to approximate any function in $C^1(\mathbb{S}^2)$ when the size $|\Delta|$ of the triangulation decreases to zero. See [25,26,33] for the results on approximation by spherical splines.

A classic approach to find an interpolating spline is to minimize an energy functional subject to interpolating and smoothness conditions. In this paper we additionally require that the spline solution is non-negative everywhere on the sphere whenever the given data values are non-negative. That is, let

$$\mathcal{E}(s) = \int_{\mathbb{S}^2} \left(\sum_{|\alpha|=2} |D^\alpha s_1|^2 \right) ds, \tag{1}$$

be the minimizing functional, where D^α stands for partial derivatives of order $|\alpha|$ with respect to the Cartesian coordinates $x, y, z, s_1(v) = \|v\| s \left(\frac{v}{\|v\|} \right)$ is the order 1 homogeneous extension of the spline s to $\mathbb{R}^3$. In the energy functional above, the spline extension is differentiated first, and then it is restricted back to the sphere before the integration. Let

$$\mathcal{F} := \{s \in S_d^r(\Delta) : s(v_i) = f_i, i = 1, \ldots, N, \text{ and } s(v) \geq 0, \forall v \in \mathbb{S}^2\} \tag{2}$$

be the subset of the spherical splines in $S_d^r(\Delta)$ that preserve nonnegativity and interpolate the data. Our goal is to find the spline $s \in \mathcal{F}$ minimizing the energy functional $\mathcal{E}$ defined by (1).

Since $\mathcal{E}(s)$ is a strictly convex nonnegative functional, the above minimization has a unique minimizer as long as the feasible set $\mathcal{F}$ in (2) is not empty. In Section 2 we show that $\mathcal{F} \in S_5^1(\Delta)$ is not empty on the sphere if the triangulation Δ is quasi-active. Additionally we show that $\mathcal{F}$ is not empty in the space of C^1 cubic splines over a Clough–Tocher refinement of triangulation Δ, as well as in spaces of C^1 cubic splines over triangulated convex quadrangulations. In Section 3 we discuss approximation power of the nonnegative splines. We extend the study of nonnegative interpolation problem to the range restricted interpolation problem in Section 4. The main result in this section is a sufficient condition on the coefficients of a spline that allows us to restrict the values of the spline to the given range. Finally, we outline the projected gradient method for computing the minimizers, and present numerical results in Section 5.

2. Existence of nonnegative interpolating splines

Let us begin with the concept of an active edge introduced for planar triangulations in [22]. Recall that the size of a spherical triangle $|\tau|$ is defined as the diameter of the smallest spherical cap containing τ. Throughout the paper we
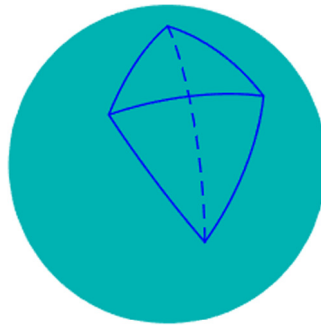
Fig. 1. The interior edge common for the two triangles is active since the arc connecting the opposite vertices (dashed line) intersects the edge.

commonly assume that the triangulation size $|\Delta| \le 1$, that is $|\tau| \le 1$ for all $\tau \in \Delta$. Let $t_1 = \langle v_1, v_2, v_3 \rangle$ and $t_2 = \langle v_2, v_4, v_3 \rangle$ be two spherical triangles in Δ having a common edge $e = \widehat{v_2, v_3}$. Under the assumption $|\Delta| \le 1$ every edge of Δ is well defined (as the shortest arc of the great circle through the two points). Additionally, the shortest arc $\widehat{v_1, v_4}$ is well defined since its length is bounded by 2. We say the edge e is *active* if the shortest arc $\widehat{v_1, v_4}$ intersects e, see Fig. 1.

Note that an edge is not active iff at one of the vertices, v_2 or v_3, the sum of interior angles is greater than π. If all angles of the triangulation are $\le \pi/2$, then all interior edges are active. Our research shows, however, that we do not need to restrict ourselves to triangulations with angles $\le \pi/2$. We can relax the requirements of active edges by introducing a new concept of quasi-active triangulation.

For a triangle $\tau \in \Delta$, let c_τ be the incenter of τ, and connect c_τ to the vertices of τ. The three triangles are called the Clough–Tocher refinement of the triangle τ, see [32] for details.

Definition 2.1. A triangulation Δ is quasi-active if any interior edge is either active or it is one of the three edges meeting at a Clough–Tocher split point.

Although the three edges connected to c_τ are not active, later in this section we establish that a nonnegative data preserving interpolating spline exists and can be constructed. We begin by describing an algorithm which converts a given triangulation into a quasi-active triangulation.

Algorithm 2.1. We convert a triangulation into a quasi-active triangulation by using the following steps. Let $\mathcal{E}$ be a list of all interior edges and $\mathcal{T}^0$ be a list of triangles. Suppose that $\mathcal{E}$ has m interior edges. For $i = 1, \ldots, m$, we do the following 4 steps:
Step 1. Write $e_i = \widehat{v_2, v_3} \in \mathcal{E}$, find the triangles $t_1 = \langle v_1, v_2, v_3 \rangle$ and $t_2 = \langle v_2, v_4, v_3 \rangle$ from $\mathcal{T}^0$ that share e_i.
Step 2. Compute the angles $\alpha = \angle v_1, v_2, v_4$ and $\beta = \angle v_1, v_3, v_4$.
Step 3. If $\alpha \le \pi$ and $\beta \le \pi$, the edge e_i is active. Define $\mathcal{T}^i = \mathcal{T}^{i-1}$, increment i by 1 and examine the next edge by going to Step 1.
Step 4. Otherwise, choose the incenter of t_1 to split t_1 into three triangles using the Clough–Tocher method and similarly, split t_2 into three subtriangles at the incenter of t_2 by the Clough–Tocher method. Define $\mathcal{T}^i$ as $\mathcal{T}^{i-1}$ with t_1, t_2 replaced by the 6 newly created triangles. Increment i by 1 and examine the next interior edge in $\mathcal{E}$ by going to Step 1.
End the do loop. Let $\widetilde{\Delta}$ be the resulting collection $\mathcal{T}^m$ of triangles.

Note that in Step 4 of Algorithm 2.1, the edge e_i becomes active according to Lemma 4.19 of [32]. Also, the other edges of t_1 and t_2 remain active if they were active before. It is easy to see that the modified triangulation $\widetilde{\Delta}$ is a quasi-active triangulation.

We now reformulate our nonnegative data preserving interpolation problem as follows.

Problem 2.1. Let Δ be a triangulation of the unit sphere and let $V = \{v_i, i = 1, \ldots, N\}$ be a subset of the vertices of Δ. Let I be a set of indices such that $\{f_i, i \in I\}$ is a data value available at $v_i \in V$. Find a spline $s_f \in S_d^r(\widetilde{\Delta})$, interpolating f_i at $v_i, i \in I$, non-negative everywhere on the unit sphere, and minimizing the functional (1), where $\widetilde{\Delta}$ is the quasi-active refinement of Δ defined by the Algorithm 2.1.

We can see that the new formulation is similar to the one presented previously. The only difference is that we allow the possibility that the spline solution interpolates the data values over a subset of vertices of $\widetilde{\Delta}$.

Let us explain how to solve Problem 1 in the setting of spherical splines of degree 3 and smoothness 1 first.

Theorem 2.2. *Let $\widetilde{\Delta}$ denote a Clough–Tocher refinement of a triangulation Δ with in-centers as split points and such that $|\Delta| \le 1$. A set of non-negative splines in $S_3^1(\widetilde{\Delta})$ interpolating non-negative data at the vertices of Δ is not empty. Therefore there exists a unique non-negative spline $S_f \in S_3^1(\widetilde{\Delta})$ minimizing (1).*
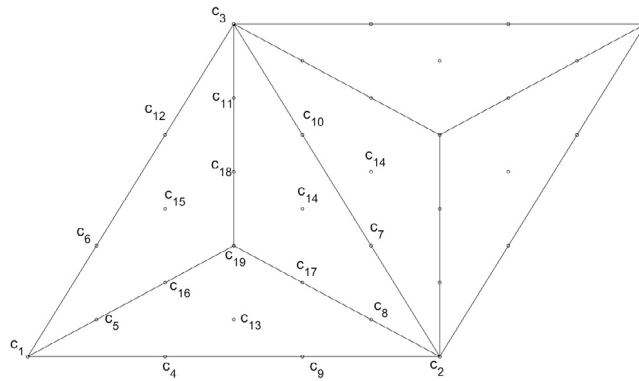
Fig. 2. Bernstein–Bézier coefficients of a cubic spline defined over a Clough–Tocher triangle.

Proof. Without loss of generality, we may assume that the values are given at all vertices of Δ, otherwise we can define the missing values to be zeros. Let τ_1 be a triangle in Δ with vertices v_1, v_2, v_3 and the in-center u_1. Let τ_2 be a triangle in Δ with vertices v_4, v_3, v_2 and the in-center u_2. Let f_i denote a value to be interpolated at v_i, for every vertex v_i of Δ. Let us assign the values of the BB-coefficients on τ_1, depicted in Fig. 2, as follows. First of all, the conditions $c_1 = f_1, c_2 = f_2, c_3 = f_3$ guarantee the interpolation at the vertices of Δ. Setting $\nabla s(v_i) = 0, i = 1, 2, 3$ preserves positivity (non-negativity) of the spline and ensures C^1 smoothness at the vertices. In this case the coefficients are computed as

$$c_4 = f_1 \langle v_1, v_2 \rangle,$$
$$c_5 = f_1 \langle v_1, u_1 \rangle,$$
$$c_6 = f_1 \langle v_1, v_3 \rangle,$$

in the first ring of the vertex v_1,

$$c_7 = f_2 \langle v_2, v_3 \rangle,$$
$$c_8 = f_2 \langle v_2, u_1 \rangle,$$
$$c_9 = f_2 \langle v_2, v_1 \rangle,$$

in the first ring of the vertex v_2, and

$$c_{10} = f_3 \langle v_3, v_1 \rangle,$$
$$c_{11} = f_3 \langle v_3, u_1 \rangle,$$
$$c_{12} = f_3 \langle v_3, v_2 \rangle,$$

in the first ring of the vertex v_3. Let us note that $|\Delta| \leq 1$ ensures that all involved dot products above are positive.

Next we enforce the only remaining C^1 condition across the edge $\widehat{v_2, v_3}$ while requiring that the coefficient c_{14} in τ_1 is equal to the corresponding coefficient of τ_2. Let (α, β, γ) denote the barycentric coordinates of u_2 with respect to $\langle v_2, v_3, u_1 \rangle$. Since the edge $\widehat{v_2, v_3}$ is active, $\alpha > 0, \beta > 0, \gamma < 0$. Then

$$c_{14} = \frac{\alpha f_2 + \beta f_3}{1 - \gamma} \langle v_2, v_3 \rangle > 0.$$

Similarly we can compute $c_{13} > 0$ and $c_{15} > 0$. Let $b_i, i = 1, 2, 3$ denote the barycentric coordinates of the in-center u_1 with respect to τ_1. Then

$$c_{16} = b_1 c_5 + b_2 c_{13} + b_3 c_{15},$$

and c_{16} is positive since b_i's are positive for any point interior to τ_1. The same holds for $c_i, i = 17, 18, 19$, and we conclude that the set of non-negative splines in $S_3^1(\widetilde{\Delta})$ interpolating non-negative data at the vertices of Δ is not empty. ∎

Theorem 2.3. *Let $r = 1$ and $d \geq 5$ be an odd integer. The set of non-negative splines in $S_d^r(\widetilde{\Delta})$ interpolating non-negative data at $V_I \subset V$ is not empty, where $\widetilde{\Delta}$ is a quasi-active triangulation obtained by using Algorithm 2.1 from some triangulation with $|\Delta| \leq 1$. Therefore there exists a unique spline $S_f \in S_d^r(\widetilde{\Delta})$ minimizing (1).*

Proof. Let τ be a triangle in Δ. When $\widetilde{\Delta}$ is constructed, the triangle τ is either preserved, if all of its edges are active, or it is split, if one or more of its edges is not active.
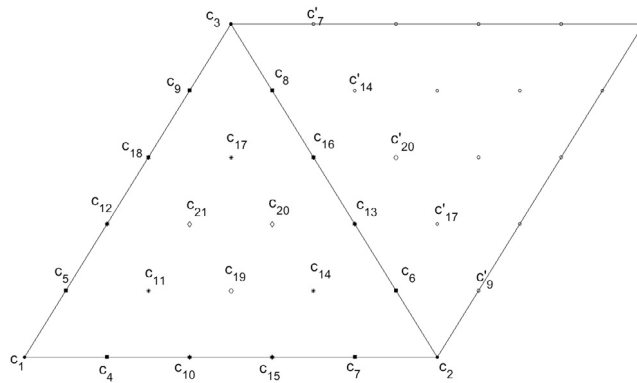
Fig. 3. Bernstein–Bézier coefficients of a quintic spline.

Consider the first possibility. That is we have $\tau \in \widetilde{\Delta}$ with all three edges being active. To define a nonnegative C^1 quintic spline over the $\tau = \langle v_1, v_2, v_3 \rangle$ and its neighboring triangles, for example $\tau' = \langle v_4, v_3, v_2 \rangle$, follow the spline coefficients over the triangles presented in Fig. 3. To interpolate the given function values f_i, $i = 1, 2, 3$ at the vertices of τ we set, as expected, $c_i = f_i$, $i = 1, 2, 3$.

Define $\delta_{ij} = \langle v_i, v_j \rangle$ to be the dot product of vectors v_i and v_j and note that $\delta_{ij} = \delta_{ji} > 0$ for every edge of a triangulation Δ since $|\Delta| \leq 1$. Consider the domain points in the first ring of v_1. We set the coefficients $c_4 = f_1 \delta_{12}$ and $c_5 = f_1 \delta_{13}$ to satisfy $\nabla s(v_1) = 0$. The coefficients in the second ring of v_1 are set to $c_{10} = f_1 \delta_{12}^2$, $c_{11} = f_1 \delta_{12} \delta_{13}$, $c_{12} = f_1 \delta_{13}^2$ to satisfy $D_{xx} s(v_1) = D_{xy} s(v_1) = D_{yy} s(v_1) = 0$. Similarly we set the coefficients in the second disks of v_i, $i = 2, 3$.

Before we proceed with defining c_i, $i = 19, 20, 21$, let us note that all the coefficients introduced so far are nonnegative if and only if f_i, $i = 1, 2, 3$ are nonnegative. To check C^1 conditions along the edge $\widehat{v_2, v_3}$ recall that

$$v_4 = b_1 v_1 + b_2 v_2 + b_3 v_3,$$

where b_i, $i = 1, 2, 3$ are the spherical barycentric coordinates of v_4 with respect to τ. It follows that

$$\langle v_4, v_3 \rangle = b_1 \langle v_1, v_3 \rangle + b_2 \langle v_2, v_3 \rangle + b_3 \langle v_3, v_3 \rangle,$$

and therefore

$$f_3 \delta_{34} = b_1 f_3 \delta_{13} + b_2 f_3 \delta_{23} + b_3 f_3,$$

which can be recognized as

$$c'_7 = b_1 c_9 + b_2 c_8 + b_3 c_3,$$

a C^1 condition across the edge $\widehat{v_2, v_3}$ near the vertex v_3. Multiply the last equation by δ_{32} to get one more C^1 condition across the edge $\widehat{v_2, v_3}$:

$$c'_{14} = f_3 \delta_{34} \delta_{32} = b_1 f_3 \delta_{13} \delta_{32} + b_2 f_3 \delta_{32}^2 + b_3 f_3 \delta_{32} = b_1 c_{17} + b_2 c_{16} + b_3 c_8.$$

Furthermore, when

$$v_4 = b_1 v_1 + b_2 v_2 + b_3 v_3$$

is dot-multiplied with v_2 we get

$$\langle v_4, v_2 \rangle = b_1 \langle v_1, v_2 \rangle + b_2 \langle v_2, v_2 \rangle + b_3 \langle v_3, v_2 \rangle,$$

and therefore

$$c'_9 = f_2 \delta_{24} = b_1 f_2 \delta_{12} + b_2 f_2 + b_3 f_2 \delta_{23} = b_1 c_7 + b_2 c_2 + b_3 c_6.$$

Moreover

$$c'_{17} = f_2 \delta_{24} \delta_{23} = b_1 f_2 \delta_{12} \delta_{23} + b_2 f_2 \delta_{23} + b_3 f_2 \delta_{23}^2 = b_1 c_{14} + b_2 c_6 + b_3 c_{13}$$

hold as well.

At last, to set up the only remaining C^1 condition across the edge $\widehat{v_2, v_3}$ define c_{20} to satisfy

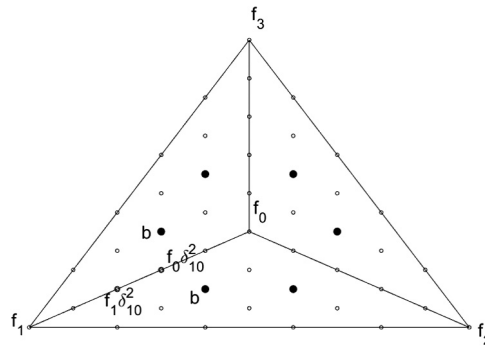$$c_{20} = b_1 c'_{20} + b_2 f_2 \delta_{32}^2 + b_3 f_3 \delta_{32}^2.$$

Fig. 4. Bernstein–Bézier coefficients of a quintic spline defined over a Clough–Tocher triangle.

It suffices to require that $c_{20} = c'_{20}$ to end up with a positive value for both

$$c_{20} = c'_{20} = \frac{b_2 f_2 + b_3 f_3}{1 - b_1} \delta_{32}^2.$$

Indeed, since the edge $\widehat{v_2, v_3}$ of τ is active, v_4 lies in the region of the unit sphere defined by $b_2(v) \geq 0, b_3(v) \geq 0, b_1(v) < 0$, where $b_i(v), i = 1, 2, 3$ are the barycentric coordinates of v with respect to τ. Note that b_2 and b_3 cannot both be zero, and therefore if f_2, f_3 are nonnegative, so are c_{20} and c'_{20}.

In the second case, τ is a triangle similar to the one shown in Fig. 4. Let f_0 be the $\max\{f_1, f_2, f_3\}$. Follow the ideas outlined above to define the coefficients of the spline on each of the sub-triangles of τ, using f_0 for the coefficients in the second disk around the split point v_0. Just like in the case of a non-split triangle, the coefficients in the second discs around $v_i, i = 0, 1, 2, 3$, as well as those involved in C^1 conditions across the outer edges of τ are nonnegative, and the spline is smooth. Now we show that the remaining coefficients, corresponding to the black dots in Fig. 4, are nonnegative as well, even though the interior edges $\widehat{v_0, v_i}, i = 1, 2, 3$ are not active. Consider for example the C^1 condition across the edge $\widehat{v_0, v_1}$ that involves b

$$f_0 \delta_{10}^2 = b_1 f_1 \delta_{10}^2 + b_2 b + b_3 b,$$

and therefore

$$b = \frac{f_0 - b_1 f_1}{b_2 + b_3} \delta_{10}^2.$$

Here $b_i, i = 1, 2, 3$ are the spherical barycentric coordinates of v_0 with respect to $\langle v_1, v_2, v_3 \rangle$, and $\delta_{10} = \langle v_1, v_0 \rangle > 0$. Since $0 < b_i < 1, b_2 + b_3 > 0$, and $f_0 = \max\{f_1, f_2, f_3\} > f_1 > b_1 f_1$.

On the sphere a quintic polynomial belongs to a space of polynomials of any odd degree greater than or equal to five. Therefore any space $S_d^1(\widetilde{\Delta}), d \geq 5$ odd, contains a non-negative spline interpolating non-negative data at the vertices of Δ. ∎

Finally we can comment on the existence of nonnegative data preserving interpolating C^1 cubic splines over triangulated convex quadrangulations. All edges of triangles interior to quadrangles are active since the interior angles of the quadrangles are strictly less than π. For an edge e shared by quadrangles Q_1 and Q_2 observe that e is active if the intersection of the diagonals of Q_2 lies between the extensions of the diagonals of Q_1. See Fig. 5 for an example of an inactive edge. It is clear that for a triangulated quadrangulation it is not enough for the original quadrangulation to be convex. We need additional constraints described above to have active triangulated quadrangulations.

Theorem 2.4. *Let Δ denote a triangulation obtained from a convex quadrangulation $\diamondsuit$ of the unit sphere by adding the two diagonals of each quadrilateral in $\diamondsuit$. Suppose that all edges of Δ are active. The set of non-negative splines in $S_3^1(\Delta)$ interpolating non-negative data at the set of vertices of the $\diamondsuit$ is not empty. Therefore there exists a unique spline $S_f \in S_3^1(\Delta)$ minimizing* (1).

Proof. The elements in the proof are similar to the ones discussed in Theorems 2.2 and 2.3 and we leave it to the interested reader. ∎

3. Approximation properties of nonnegative interpolating splines

Let S_f be the nonnegative preserving interpolating spline constructed in the previous section. Let us study approximation properties of S_f in this section. Let $W^{2,\infty}(\mathbb{S}^2)$ be the Sobolev-type space of spherical functions with the derivatives of order
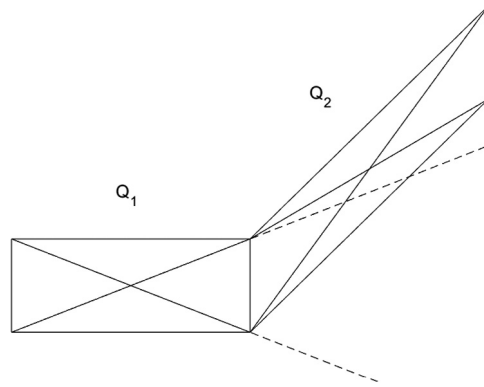
Fig. 5. An inactive edge shared by Q_1 and Q_2: the intersection of the diagonals of Q_2 is not between the extensions of the diagonals of Q_1.

two or less bounded with respect to maximum norm. Recall that a semi-norm can be defined on $W^{2,\infty}(\mathbb{S}^2)$ as

$$|f|_{2,\infty,\mathbb{S}^2} = \sum_{t\in\Delta}\sum_{|\alpha|=2}\|D^\alpha f_1\|_{\infty,t}.$$

Recall the following approximation property (Theorem 2 in [25]).

Theorem 3.1. *Let Δ be a β-quasi-uniform spherical triangulation with $|\Delta| \leq 1$. Let $1 \leq p \leq \infty$, $d \geq 3r + 2$, and $0 \leq k \leq d$. There exists a quasi-interpolating operator Q mapping $f \in C(\mathbb{S}^2)$ into $S_d^r(\Delta)$ such that Qf achieves the optimal approximation order. That is for all $f \in W^{m+1,p}(\mathbb{S}^2)$ with $Qf \in W^{k,p}(\mathbb{S}^2)$*

$$|f - Qf|_{k,p,\mathbb{S}^2} \leq C|\Delta|^{m+1-k}|f|_{m+1,p,\mathbb{S}^2}$$

Here $0 \leq m \leq d$, and $(d - m) \bmod 2 = 0$. The constant C depends on the degree d, p, and the smallest angle θ_Δ.

Theorem 3.2. *Suppose $f_i = f(v_i)$, $i = 1, \ldots, n$ for a smooth positive function $f \in W^{2,\infty}(\mathbb{S}^2)$. Let $d \geq 3r + 2$ be an odd integer and let Δ be a triangulation of the data sites $\{v_i, i = 1, \ldots, N\}$ with $|\Delta| \leq 1$. Let S_f denote a spline in $S_d^r(\Delta)$ minimizing (1) over the set*

$$U_f := \{s \in S_d^r(\Delta) : s(v_i) = f_i, i = 1, \ldots, N, \text{ and } s(v) \geq 0, \forall v \in \mathbb{S}^2\}.$$

Then

$$\|S_f - f\|_{2,\mathbb{S}^2} \leq C|\Delta|^2|f|_{2,\infty,\mathbb{S}^2},$$

where $C > 0$ is a constant dependent on d, and the smallest angle of Δ.

Proof. Since f is positive over $\mathbb{S}^2$, let us say $f \geq \epsilon > 0$ on $\mathbb{S}^2$. For every $\tau \in \Delta$ by Lemma 7 in [25], since f and S_f are equal at the vertices of τ, we have

$$\|S_f - f\|_{\infty,\tau} \leq C|\tau|^2|S_f - f|_{2,\infty,\tau} \leq C|\tau|^2\left(|f|_{2,\infty,\tau} + |S_f|_{2,\infty,\tau}\right).$$

According to Lemma 4.4 in [33] there exists a positive constant K depending on d, and the smallest angle of τ, such that

$$A_\tau^{-1/2}\|p\|_{2,\tau} \leq \|p\|_{\infty,\tau} \leq KA_\tau^{-1/2}\|p\|_{2,\tau}, \tag{3}$$

for any trivariate homogeneous polynomial p of degree d, A_τ stands for the area of τ. By (3) and Lemma 10 in [25]

$$|S_f|_{2,\infty,\tau} \leq KA_\tau^{-1/2}|S_f|_{2,2,\tau} \leq K'A_\tau^{-1/2}\left(\mathcal{E}_\tau(S_f)\right)^{1/2},$$

where $\mathcal{E}_\tau$ is the energy functional (1) evaluated on τ. Since for any point $v \in \mathbb{S}^2$,

$$f(v) - Qf(v) \leq \|f - Qf\|_{\infty,\mathbb{S}^2}$$

and $f \geq \epsilon > 0$ we have

$$Qf(v) \geq f(v) - \|f - Qf\|_{\infty,\mathbb{S}^2} \geq \epsilon - C|\Delta|^{m+1}|f|_{m+1,\infty,\mathbb{S}^2}.$$

It follows that when $|\Delta|$ is small enough $Qf \geq 0$. Since Qf interpolates f at the vertices of Δ, it belongs to the set of nonnegative interpolating splines U_f defined above, and thus $\mathcal{E}(S_f) \leq \mathcal{E}(Qf)$. By Lemma 10 in [25] and (3)

$$\mathcal{E}(Qf) \leq |Qf|_{2,2,\mathbb{S}^2}^2 = \sum_{\tau\in\Delta}|Qf|_{2,2,\tau}^2 \leq \sum_{\tau\in\Delta}A_\tau|Qf|_{2,\infty,\tau}^2 \leq 4\pi|Qf|_{2,\infty,\mathbb{S}^2}^2.$$

Then

$$\mathcal{E}(S_f) \leq \mathcal{E}(Qf) \leq 4\pi |Qf|^2_{2,\infty,\mathbb{S}^2}$$
$$\leq 8\pi |Qf - f|^2_{2,\infty,\mathbb{S}^2} + 8\pi |f|^2_{2,\infty,\mathbb{S}^2} \leq 8\pi (C^2+1)|f|^2_{2,\infty,\mathbb{S}^2}$$

by Theorem 2.4 with $m + 1 = k = 2$. Summarized the discussion above, we have

$$
\begin{aligned}
\|S_f - f\|^2_{2,\mathbb{S}^2} &= \sum_{\tau \in \Delta} \int_\tau |S_f - f|^2 ds \leq \sum_{\tau \in \Delta} A_\tau \|S_f - f\|^2_{\infty,\tau} \\
&\leq \sum_{\tau \in \Delta} A_\tau 2C^2 |\tau|^4 \left(|f|^2_{2,\infty,\tau} + K'^2 A_\tau^{-1} \mathcal{E}_\tau(S_f) \right) \\
&\leq 2C^2 |\Delta|^4 \sum_{\tau \in \Delta} A_\tau |f|^2_{2,\infty,\mathbb{S}^2} + 2C^2 K'^2 |\Delta|^4 \sum_{\tau \in \Delta} \mathcal{E}_\tau(S_f) \\
&\leq 8\pi C^2 |\Delta|^4 |f|^2_{2,\infty,\mathbb{S}^2} + 2C^2 K'^2 |\Delta|^4 \mathcal{E}(S_f) \\
&\leq 8\pi C^2 |\Delta|^4 |f|^2_{2,\infty,\mathbb{S}^2} + 2C^2 K'^2 |\Delta|^4 8\pi (C^2+1)|f|^2_{2,\infty,\mathbb{S}^2} \\
&= \left(8\pi C^2 + 16\pi C^2 K'^2 (C^2+1) \right) |\Delta|^4 |f|^2_{2,\infty,\mathbb{S}^2}
\end{aligned}
$$

Thus we have completed the proof. ∎

To prove similar results in C^1 cubic spline spaces over triangulated quadrangulations and Clough–Tocher triangulations we first recall Theorems 6.6 and 6.18 in [32]. One can extend these results to the spherical setting straightforwardly. Let us write the spherical extension as follows.

Theorem 3.3. *Let $\mathcal{S}$ be a spherical spline space of degree 3 over either a spherical triangulated quadrangulation or over the Clough–Tocher refinement of a spherical triangulation. Assume that every macro-triangle or macro-quadrilateral $|\tau| \leq 1$. Let $\mathcal{I}$ be the Hermite interpolating operator, i.e. $\mathcal{I}f$ interpolates f and its first order derivatives at the respective nodes, and let $1 \leq m \leq 3$ with $m = 3mod(2)$. Then for all $f \in W^{m+1,\infty}(\mathbb{S}^2)$*

$$|f - \mathcal{I}f|_{k,\infty,\Omega} \leq C|\Delta|^{m+1-k}|f|_{m+1,\infty,\Omega},$$

for all $0 \leq k \leq m$. If Ω covers $\mathbb{S}^2$, the constant C depends on the smallest angle of Δ. Otherwise K may depend on the boundary $\partial\Omega$ of Ω.

Similar to Theorem 3.2, we can establish the following

Theorem 3.4. *Suppose $f_i = f(v_i)$, $i = 1, \ldots, n$ for a smooth positive function $f \in W^{4,\infty}(\mathbb{S}^2)$. where $\{v_i, i = 1, \ldots, N\}$ are vertices of macro-triangles, with $|\Delta| \leq 1$. Let S_f denote a spline in $\mathcal{S}$, a C^1 cubic spherical spline space over a Clough–Tocher refinement of Δ or a triangulated quadrangulation, minimizing (1) over the set*

$$U_f := \{s \in \mathcal{S} : s(v_i) = f_i, i = 1, \ldots, N, \text{ and } s(v) \geq 0, \forall v \in \mathbb{S}^2\}.$$

Then

$$\|S_f - f\|_{2,\mathbb{S}^2} \leq C_1 |\Delta|^2 |f|_{2,\infty,\mathbb{S}^2} + C_2 |\Delta|^4 |f|_{4,\infty,\mathbb{S}^2},$$

where $C > 0$ is a constant dependent the smallest angle of the underlying triangulation.

Proof. The ideas of the proof are exactly the same as the one for Theorem 3.2. We omit the detail. ∎

4. Range restricted interpolation

The non-negativity constraint can be extended to a problem of range restricted interpolation. That is, Problem 1 in the previous section can be extended as follows.

Problem 4.1. Suppose the given data are bounded $a \leq f_i \leq b$, $i = 1, \ldots, N$. Find a spline function $s \in S^r_d(\Delta)$ that interpolates the given data and such that $a \leq s(v) \leq b$, $\forall v \in \mathbb{S}^2$.

In this section we consider the following constrained minimization:

$$\min \mathcal{E}(s), s \in \mathcal{F}_{a,b}, \tag{4}$$

where

$$\mathcal{E}(s) = \int_{\mathbb{S}^2} \left(\sum_{|\alpha|=2} |D^\alpha s_1|^2 \right) ds,$$

and

$$\mathcal{F}_{a,b} := \{s \in S_d^r(\Delta) : s(v_i) = f_i, i = 1, \ldots, N, \text{ and } a \le s(v) \le b, \forall v \in \mathbb{S}^2\}$$

is the feasible set in spherical spline space $S_d^r(\Delta)$.

To solve Problem 2, we convert the range restriction on spline functions to the range restriction on their coefficients. To this purpose we begin with

Lemma 4.1. *Let $|\tau|$ denote the size of a spherical triangle τ, and assume that $|\tau| \le 1$. The sum of spherical homogeneous Bernstein–Bézier basis polynomials of degree d with respect to τ satisfies*

$$\max_{v \in \tau} \left(\sum_{i+j+k=d} B_{ijk}^d(v) \right) \le \frac{1}{(\cos(|\tau|/2))^d}.$$

Proof. Let $\tau = \langle v_1, v_2, v_3 \rangle$ be a spherical triangle with $|\tau| \le 1$. Let $\bar{\tau}$ denote the planar triangle with the same vertices and belonging to the plane determined by the vertices $v_i, i = 1, 2, 3$. Notice that for every $\bar{v} \in \bar{\tau}$ the map $\phi(\bar{v}) = \bar{v}/\|\bar{v}\| = v$ defines the radial projection of $\bar{v}$ onto τ. The planar barycentric coordinates $\bar{b}_i$ of $\bar{v}$ with respect to $\bar{\tau}$ can be related to the spherical barycentric coordinates $b_i(v)$ with respect to τ as follows. For every $v \in \tau$ the spherical barycentric coordinates satisfy

$$\sum_{i=1}^3 b_i(v)v_i = v = \frac{\bar{v}}{\|\bar{v}\|},$$

where $\bar{v}$ is uniquely defined by the inverse of the radial projection map ϕ. Multiply both sides of the above by $\|\bar{v}\|$ to get

$$\sum_{i=1}^3 \|\bar{v}\|b_i(v)v_i = \bar{v}.$$

It is not too difficult to check that $\|\bar{v}\|b_i(v), i = 1, 2, 3$ are the planar barycentric coordinates of $\bar{v}$ with respect to $\bar{\tau}$. Next we relate the spherical homogeneous Bernstein–Bézier (BB) basis polynomials of degree d on τ to the planar BB basis polynomials of degree d on $\bar{\tau}$:

$$\bar{B}_{ijk}^d(\bar{v}) = \frac{d!}{i!j!k!} \bar{b}_1^i(\bar{v})\bar{b}_2^j(\bar{v})\bar{b}_3^k(\bar{v}) = \|\bar{v}\|^d \frac{d!}{i!j!k!} b_1^i(v)b_2^j(v)b_3^k(v) = \|\bar{v}\|^d B_{ijk}^d(v).$$

We can now conclude that

$$\sum_{i+j+k=d} B_{ijk}^d(v) = \frac{1}{\|\bar{v}\|^d} \sum_{i+j+k=d} \bar{B}_{ijk}^d(\bar{v}) = \frac{1}{\|\bar{v}\|^d}.$$

In general $\|\bar{v}\| \le 1$, and thus

$$\sum_{i+j+k=d} B_{ijk}^d(v) \ge 1.$$

For our purposes however we would like to analyze the dependence of $\|\bar{v}\|$ on the size of τ. Notice that the smallest value of $\|\bar{v}\|$ is the distance from the origin to the plane defined by $\bar{\tau}$. View the vertices of $\bar{\tau}$ as the base of a triangular pyramid with the edge lengths from the origin to the base all equal to 1. The foot of the altitude dropped from the origin to the base lies at the center of the circle out-scribing $\bar{\tau}$. The projection of the foot onto the sphere is the center of the smallest spherical cap containing τ, and thus the angle between any of the vectors $v_i, i = 1, 2, 3$ and the altitude is $|\tau|/2$. Therefore the length of the altitude and therefore the smallest value of $\|\bar{v}\|$ on $\bar{\tau}$ is $\cos(|\tau|/2)$. ∎

Lemma 4.2. *Let $|\tau|$ denote the size of a spherical triangle τ, and suppose that $|\tau| \le 1$. Let $d \ge 2$ denote the degree of spherical homogeneous BB-basis polynomials. Let $\mathcal{I}$ denote the index set of triples $(d, 0, 0), (0, d, 0), (0, 0, d)$ and $\mathcal{J}$ denote the set of indices of triples $(i, j, k), i + j + k = d$ that are not in $\mathcal{I}$. There exists a constant $0 < K < 1$ depending on $|\tau|$ and d such that*

$$\sum_{\mathcal{I}} B_{ijk}^d(v) + K \sum_{\mathcal{J}} B_{ijk}^d(v) \le 1 \tag{5}$$

for any point $v \in \tau$.

Proof. We begin the proof with the case $d = 2$. Recall that (Lemma 13.7 in [32]) for spherical barycentric coordinates

$$b_1^2 + b_2^2 + b_3^2 + 2\cos(\alpha)b_1b_2 + 2\cos(\beta)b_2b_3 + 2\cos(\gamma)b_1b_3 = 1,$$

where α is the lengths of the edge $\widehat{v_1, v_2}$ in τ. Since $\alpha \leq |\tau|$, $\cos(\alpha) \geq \cos(|\tau|)$, and similarly for β and γ. Then

$$b_1^2 + b_2^2 + b_3^2 + \cos(|\tau|)(2b_1b_2 + 2b_2b_3 + 2b_1b_3)$$
$$\leq b_1^2 + b_2^2 + b_3^2 + 2\cos(\alpha)b_1b_2 + 2\cos(\beta)b_2b_3 + 2\cos(\gamma)b_1b_3 = 1,$$

and thus (5) holds with $K = \cos(|\tau|)$, where $0 < \cos(|\tau|) < 1$ as desired.

Next we consider the case of degree $d = 3$. Recall that for a point v in τ, $b_i(v) \leq 1$, $i = 1, 2, 3$. Then

$$\sum_{\mathcal{I}} B_{ijk}^3(v) + K \sum_{\mathcal{J}} B_{ijk}^3(v) =$$

$$\sum_{i=1}^{3} b_i^3 + 3K(b_1^2 b_2 + b_1 b_2^2) + 3K(b_1^2 b_3 + b_1 b_3^2) + 3K(b_3^2 b_2 + b_3 b_2^2) +$$

$$2K(3b_1 b_2 b_3) \leq \sum_{i=1}^{3} b_i^2 + 3K(2b_1 b_2) + 3K(2b_1 b_3) + 3K(2b_3 b_2) +$$

$$2K(b_1 b_2 + b_1 b_3 + b_2 b_3) = \sum_{i=1}^{3} b_i^2 + 4K(2b_1 b_2 + 2b_1 b_3 + 2b_2 b_3) \leq 1$$

with $K = \cos(|\tau|)/4$ and using the result for $d = 2$.

Finally, let us treat the case $d \geq 4$. Let $\mathcal{K}$ denote the set of triples (i, j, k) such that neither index is zero. Then

$$\sum_{\mathcal{I}} B_{ijk}^d(v) + K \sum_{\mathcal{J}} B_{ijk}^d(v) =$$

$$\sum_{i=1}^{3} b_i^d + K \sum_{i=1}^{d-1} \binom{d}{i} b_1^i b_2^{d-i} + K \sum_{j=1}^{d-1} \binom{d}{j} b_2^j b_3^{d-j} +$$

$$K \sum_{k=1}^{d-1} \binom{d}{k} b_3^k b_1^{d-k} + K \sum_{\mathcal{K}} \frac{d!}{i!j!k!} b_1^i b_2^j b_3^k.$$

Denote $A = \sum_{i=1}^{d-1} \binom{d}{i}$ and $B = \sum_{\mathcal{K}} \frac{d!}{i!j!k!}$. Then using $b_i < 1$, $i = 1, 2, 3$ as needed

$$\sum_{\mathcal{I}} B_{ijk}^d(v) + K \sum_{\mathcal{J}} B_{ijk}^d(v) \leq$$

$$\sum_{i=1}^{3} b_i^2 + KA(b_1 b_2 + b_2 b_3 + b_3 b_1) + KB b_1 b_2 b_3 \leq$$

$$\sum_{i=1}^{3} b_i^2 + KA(b_1 b_2 + b_2 b_3 + b_3 b_1) + KB/3(b_1 b_2 + b_2 b_3 + b_1 b_3) =$$

$$\sum_{i=1}^{3} b_i^2 + K(A + B/3)(b_1 b_2 + b_2 b_3 + b_3 b_1) \leq 1,$$

with $K = 2\cos(|\tau|)/(A + B/3)$ and using the result for $d = 2$. ∎

Theorem 4.3. *Let τ be a spherical triangle with $|\tau| \leq 1$. Let p be a spherical homogeneous Bernstein–Bézier polynomial p of degree d on the triangle τ. Write $\mathbf{c} = \{c_{ijk}, i + j + k = d\}$ to be the vector of the coefficients of p. Let $\mathcal{I}, \mathcal{J}$ be the subsets of triple indices defined in Lemma 4.2. Suppose $a < b$ are strictly positive. If*

$$a \leq c_{ijk} \leq b, (i, j, k) \in \mathcal{I},$$

and

$$a \leq c_{ijk} \leq Kb, (i, j, k) \in \mathcal{J},$$

then

$$a \leq p(v) \leq b$$

for all $v \in \tau$, where K is the constant defined in Lemma 4.2 depending on d and $|\tau|$.

Proof. Using Lemma 4.2,

$$p(v) = \sum_{i+j+k=d} c_{ijk} B_{ijk}^d(v) = \sum_{\mathcal{I}} c_{ijk} B_{ijk}^d(v) + \sum_{\mathcal{J}} c_{ijk} B_{ijk}^d(v)$$

$$\leq b \sum_{\mathcal{I}} B_{ijk}^d(v) + b \sum_{\mathcal{J}} K B_{ijk}^d(v) \leq b,$$

for every $v \in \tau$.

On the other hand, since the sum of spherical homogeneous BB-basis polynomials is greater than or equal to one

$$p(v) = \sum_{i+j+k=d} c_{ijk} B_{ijk}^d(v) \geq a \sum_{i+j+k=d} B_{ijk}^d(v) \geq a.$$

We have thus completed the proof.   ■

These constraints will be used in our computation to find the range restricted data interpolating spline. That is, for a given triangulation and a spline degree we first compute $K = K(t)$, $t \in \Delta$. Then we define $a := \min_{1 \leq i \leq N}\{f_i\}$ and $b := \max_{1 \leq i \leq N}\{f_i\}$ for the given data f_i, $i = 1, \ldots, N$. Let

$$\mathcal{B}_{a,b} :=$$
$$\{s \in S_d^r(\Delta) : s(v_i) = f_i, i = 1, \ldots, N, a \leq c_{ijk}^t \leq K(t)b, (ijk) \in \mathcal{J}, t \in \Delta\}$$

be a new feasible set in a spherical spline space $S_d^r(\Delta)$. Instead of (4), we solve the following constrained minimization problem:

$$\min \mathcal{E}(s), s \in \mathcal{B}_{a,b}. \tag{6}$$

As long as the feasible set is not empty, the above minimization has a unique solution. The proof in Section 2 can be adapted to show that the $\mathcal{B}_{a,b}$ is not empty in $S_3^1(\widetilde{\Delta})$, where $\widetilde{\Delta}$ is the Clough–Tocher refinement of Δ as described in Section 2. Convergence of range restricted splines can be established as well. We leave these considerations to the interested reader.

With the above preparation, we now use the projected gradient method to solve the above minimization problem (6). Note that $\mathcal{E}(s) = \mathcal{E}(\mathbf{c})$ can be viewed as $\mathbf{c}^T E \mathbf{c}$ where E is an energy matrix corresponding to the functional $\mathcal{E}$, and $\mathbf{c}$ is a vector of the spline coefficients. Respectively, it is easy to see that $\nabla \mathcal{E}(s) = \nabla \mathcal{E}(\mathbf{c})$ is equivalent to $2E\mathbf{c}$.

Algorithm 4.1. Starting with an initial guess $\mathbf{c}^{(0)}$, compute

$$\mathbf{c}^{(k+1)} = \mathbf{P}_{\mathcal{B}_{a,b}} \left(\mathbf{c}^{(k)} - h \nabla \mathcal{E}(\mathbf{c}^{(k)}) \right)$$

for $k \geq 0$, where $h > 0$ is a step size and $\mathbf{P}_{\mathcal{B}_{a,b}}(\mathbf{y})$ is the projection of $\mathbf{y}$ into the feasible set $\mathcal{B}_{a,b}$.

It is known [34] that the above Algorithm 4.1 converges when $\mathcal{E}$ is strongly convex. The computation of the gradient descent method can be accelerated using the technique in [35]. It is easy to verify that $\mathcal{E}$ is indeed convex. We omit the detail.

5. Numerical results

5.1. Simulation results

We implemented the projected gradient method to solve the constrained minimization problems in spherical spline spaces and tested several examples to assess their performance. The major computational step is the minimization of the quadratic functional for which we use the Lagrange multiplier method discussed in [1]. We can find the vector $\mathbf{c}^{(k+1)}$ using least squares method as the following system of linear equations is not of full rank, or applying the iterative method discussed in [1]:

$$\begin{pmatrix} I & B^\top & H^\top \\ B & 0 & 0 \\ H & 0 & 0 \end{pmatrix} \begin{bmatrix} \mathbf{c}^{(k+1)} \\ \alpha \\ \gamma \end{bmatrix} = \begin{bmatrix} \mathbf{c}^{(k)} - \mathbf{h}E\mathbf{c}^{(k)} \\ \mathbf{z} \\ 0 \end{bmatrix}$$

for Lagrange multipliers α and γ, where I is the identity matrix, B is a matrix associated with interpolating conditions, i.e. $B\mathbf{c} = \mathbf{z}$ with $\mathbf{z}$ being the vector of given function values, and H is the matrix associated with smoothness conditions. See [3] for spherical spline implementation.

Example 5.1. We begin with a simple example. Let Δ_0 be a triangulation of the unit sphere based on 6 vertices $\pm e_i$, $i = 1, 2, 3$. Let Δ_k stand for the uniform refinement of Δ_{k+1}. We use $f(x, y, z) = x^2$ as a testing function. Note that our spline spaces $S_5^1(\Delta_k)$ are not able to reproduce even degree function $f(x, y, z) = x^2$ in the spherical setting. Sample $f(x, y, z) = x^2$

Table 1
Numerical results for non-negative interpolating splines.

Level of refinement	Accuracy of Interpolation, s_+	Accuracy of Interpolation, s_m
0	7.42657e−2	7.42668e−2
1	2.22020e−2	2.22020e−2
2	1.95621e−3	1.95621e−3
3	1.43149e−4	1.43150e−4

Fig. 6. Minimal energy spline solution in Example 5.3.

at the vertices of Δ_k, $k = 0, 1, 2, 3$. Compute 1) the non-negative minimal energy interpolant s_+, and 2) the classic minimal energy interpolant s_m in $S_5^1(\Delta_k)$. Compare both interpolants to the original function with respect to ∞ norm.

In this example the tested function is nonnegative everywhere on the sphere, and both solutions are non-negative. As a result they are very close to each other, see Table 1 for details. This example shows that our MATLAB code works correctly when the minimal energy solution can be expected to be nonnegative.

Example 5.2. In this example we compare the behaviors of the minimal energy spline solution and the nonnegative spline solution generated by Algorithm 4.1 in the case when the minimal energy spline is unable to attain nonnegativity. The data are generated by evaluating $f(x, y, z) = 2(x − .5).^2 − .1$ at the vertices of Δ_0. All these values are strictly positive, in fact $f(v_i) \geq 0.4$ for every vertex v_i, $i = 1, \ldots, 6$ of Δ_0. For the minimal energy spline in $S_5^1(\Delta_0)$ evaluated at more than 5000 locations almost uniformly distributed over the sphere we have $\min(s) \approx −0.24$, while for the nonnegative spline solution evaluated at the same locations we have $\min(s_+) \approx 0.34$. The cubic spline solutions over Clough–Tocher refinement of Δ_0 have $\min(s) \approx −0.44$ and $\min(s_+) \approx 0.23$ respectively. For a quadrangulation defined over the same six vertices (plus 4 in-centers, and thus overall 16 triangles), a cubic C^1 minimal energy spline has a minimal value of $\approx −0.48$, while the positive spline solution has a minimum value of ≈ 0.01.

Example 5.3. In this example we compute a range-restricted minimal energy interpolating spline s_{rr} in $S_5^1(\Delta_3)$ for various values of the constant K of Theorem 4.3, and compare the results to the classic minimal energy interpolating spline s. We test the function

$$f(x, y, z) = e^{-\frac{x-\sin(5z)}{2-y^3}},$$

for which the values at the vertices range from 0.3751 to 2.6660. Fig. 6 shows the classic minimal energy interpolating spline evaluated at about 30,000 locations on the unit sphere. As expected, for this triangulation the spline approximates the test function quite well, in fact $\|s − f\|_\infty = 7.98e−2$. The range of values for the spline is [0.3516, 2.7671], that is both the minimal and the maximal values of this solution are outside the data range.

The results for the range-restricted solutions for various values of K are summarized in Table 2. As we decrease the value of K from 1 to 0.9 the range-restricted spline deviates from the test function more and more. Meanwhile, its maximal value decreases, and once $K \leq 0.935$ the range of s_{rr} is contained in the range for the data values. Fig. 7 illustrates visual differences between two range-restricted solutions: $K = 0.9$, left, and $K = 0.935$, right. When the coefficients of the range-restricted spline are suppressed by the constant K too much ($K = 0.9$) there is a small dent in the upper left region of the mushroom's cap. By adjusting K to 0.935, we keep the values of the spline on the right within the range (under $\max(f) = 2.666$), while improving its shape.

5.2. A real life example

One of the characteristics of atmosphere is specific humidity. By the definition specific humidity is a non-negative quantity, which makes it a good candidate for testing performance of non-negative interpolating spline. Data near the ocean surface are available on National Oceanic and Atmospheric Administration web site at
https://www.ncei.noaa.gov/data/ocean-near-surface-atmospheric-properties/access/.

Table 2
Numerical results for range-restricted interpolating splines.

K	$\|s_{rr} - f\|_\infty$	$[\min(s_{rr}), \max(s_{rr})]$
1.000	0.8066e−1	[0.3800, 2.7538]
0.960	1.2954e−1	[0.3800, 2.7029]
0.935	1.8479e−1	[0.3800, 2.6625]
0.900	2.7093e−1	[0.3800, 2.6113]

Fig. 7. Range-restricted spline solutions in Example 5.3. Left: $K = 0.9$, right: $K = 0.935$.
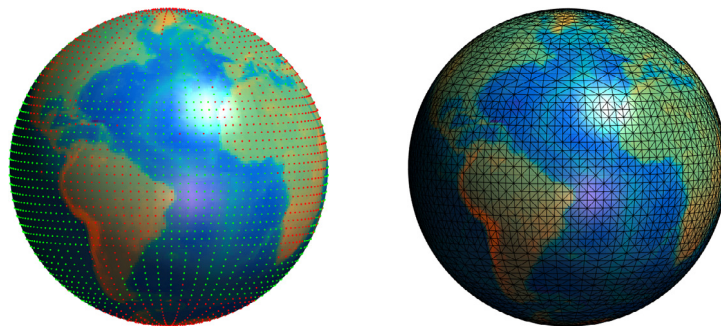

Fig. 8. Left: data locations, right: global triangulation $\triangle$.

Data are collected at three hour intervals over subsets of fixed locations on a spherical grid. For the purpose of our experiment we thinned the data, and ended up with a set of 4052 vertices and 8100 triangles over the unit sphere, see Fig. 8, left. Locations marked by red and green dots are used to construct a global triangulation, Fig. 8, right. For the first experiment the data are available at the locations marked by green dots only. We worked with the data collected on August 28–29 of 2005, conducting total of 16 experiments. The subset of available data changes from experiment to experiment, the number of data varies between 2309 and 2332.

We computed global spline solutions, C^1 minimal energy s and non-negative s_+ interpolants of degree five, thus obtaining estimates of specific humidity over the continents. After evaluating the splines at about 170,000 locations minimal values were computed for all data sets and all spline solutions. Results are summarized in Table 3. As can be seen in the table, in six out of 16 cases minimal energy splines produced negative minimal values, while s_+ spline solutions remained non-negative. The two spline solutions for the data presented in Fig. 8 are visualized in Fig. 9, the transparent surfaces are defined by triples $((1+f(x, y, z)/100)x, (1+f(x, y, z)/100)y, (1+f(x, y, z)/100)z)$ with f being the standard minimal energy spline on the left, and nonnegative spline on the right. This particular visualization shows the region on the globe where the standard minimal energy spline is negative as a portion of the spline surface buried underneath the surface of the globe. The same region on the surface visualizing the nonnegative spline lies on top of the surface of the globe.

In all of the experiments the accuracy of satisfying interpolating and smoothness conditions was of the same magnitude for all splines, and coefficient vector computational times for nonnegative spline solutions tended to be 5–6 times faster than those for standard minimal energy splines because of the iterative solutions of Algorithm 4.1 while the standard minimal energy splines are solved by a direct method.
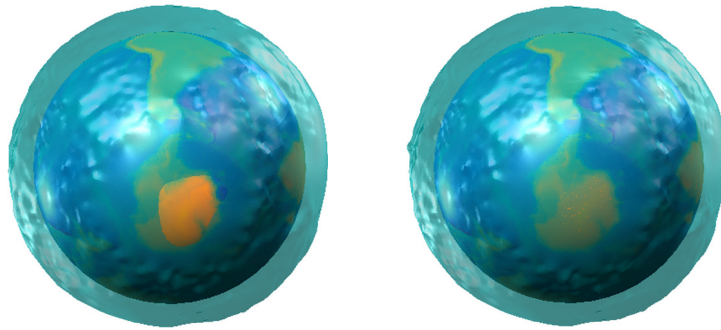
Acknowledgments

Fig. 9. Left: minimal energy interpolating spline in $S_5^1(\Delta)$ with a negative region (seen in light brown), right: nonnegative minimal energy interpolating spline in $S_5^1(\Delta)$.

Table 3
Minimal spline values, for a minimal energy spline s and a nonnegative spline s_+, versus minimal specific humidity values for 16 sets.

k	$\min(f)$	$\min(s)$	$\min(s_+)$
1	2.3681	−1.1662	0.0000
2	2.5941	−0.3296	0.0000
3	2.4993	1.0578	1.0386
4	2.3360	1.3691	1.3505
5	2.0181	1.2773	1.2789
6	1.9905	1.9305	1.9094
7	2.3136	2.2312	2.2337
8	2.2986	1.7855	1.8815
9	2.2596	0.7284	0.7071
10	2.6006	−1.1741	0.0000
11	2.5315	−0.3157	0.0000
12	2.6824	−0.8008	0.0000
13	2.4019	−0.8465	0.0000
14	2.3936	0.9652	0.9593
15	2.4218	1.6437	1.7819
16	2.4871	2.1182	2.2126

References

[1] G. Awanou, M.J. Lai, P. Wenston, Multivariate spline method for numerical solution of partial differential equations, in: G. Chen, M.J. Lai (Eds.), Wavelets and Splines, Nashboro Press, 2006, pp. 24–74.
[2] M. Lai, Multivariate splines for data fitting and approximation, in: M. Neamtu, L.L. Schumaker (Eds.), Approximation Theory XII, Nashboro Press, 2008, pp. 210–228.
[3] V. Baramidze, M.-J. Lai, C. Shum, Spherical splines for data interpolation and fitting, SIAM J. Sci. Comput. 28 (1) (2006) 241–259.
[4] M.-J. Lai, L.L. Schumaker, A domain decomposition method for computing bivariate spline fits of scattered data, SIAM J. Numer. Anal. 47 (2) (2009) 911–928.
[5] T. Zhou, D. Han, M.-J. Lai, Energy minimization method for scattered data Hermite interpolation, Appl. Numer. Math. 58 (5) (2008) 646–659.
[6] F. Utreras, Positive thin plate splines, Approx. Theory Appl. 1.3 (1985) 77–108.
[7] P. Costantini, F. Fontanella, Shape-preserving bivariate interpolation, SIAM J. Numer. Anal. 27.2 (1990) 488–506.
[8] P. Costantini, C. Manni, A local scheme for bivariate co-monotone interpolation, Comput. Aided Geom. Des. 8 (1991) 371–391.
[9] J.W. Schmidt, W. Hess, S-convex, monotone, and positive interpolation with rational bicubic splines of C2-continuity, BIT Numer. Math. 33.3 (1993) 496–511.
[10] K. Willemans, P. Dierckx, Nonnegative surface fitting with Powell-Sabin splines, Numer. Algorithms 9.2 (1995) 263–276.
[11] L.L. Schumaker, L. Han, Fitting monotone surfaces to scattered data using C^1 piecewise cubics, SIAM J. Numer. Anal. 34 (1997) 569–585.
[12] J.W. Schmidt, Range restricted interpolation by cubic C^1-splines on clough-tocher splits, Math. Res. 107 (1999) 253–268.
[13] E. Chan, B. Ong, Range restricted scattered data interpolation using convex combination of cubic Bézier triangles, J. Comput. Appl. Math. 136 (1) (2001) 135–147.
[14] J.E. Lavery, Shape preserving, multiscale interpolation by bi- and multivariate cubic L_1 splines, Comput. Aided Geom. Des. 18 (2001) 321–343.
[15] D.E. Gilsinn, J.E. Lavery, Shape preserving, multiscale fitting of bivariate data by cubic L_1 smoothing splines, in: J.S.C.K. Chui, L.L. Schumaker (Eds.), Approximation Theory X: Wavelets, Splines, and Applications, Vanderbilt University Press, Nashville, TN, 2002, pp. 283–293.
[16] A. Kouibia, M. Pasadas, Variational bivariate interpolating splines with positivity constraints, Appl. Numer. Math. 44.4 (2003) 507–526.
[17] C. Witzgall, D.E. Gilsinn, M.A. McClain, An examination of new paradigms for spline approximations, J. Res.-Natl. Inst. Standards Technol. 111.2 (2006) 57.
[18] J.M. Carnicer, T.N. Goodman, J.M. Peña", Convexity preserving scattered data interpolation using Powell-Sabin elements, Comput. Aided Geom. Design 26.7 (2009) 779–796.
[19] L.L. Schumaker, H. Speleers, Nonnegativity preserving macro-element interpolation of scattered data, Comput. Aided Geom. Des. 27.3 (2010) 245–261.
[20] L.L. Schumaker, H. Speleers, Convexity preserving splines over triangulations, Comput. Aided Geom. Des. 28.4 (2011) 270–284.

[21] M.Z. Hussain, M. Sarfraz, A. Shakeel, Shape preserving surfaces for the visualization of positive and convex data using rational bi-quadratic splines, Int. J. Comput. Appl. 27.10 (2011) 12–20.

[22] M.-J. Lai, C. Meile, Scattered data interpolation with nonnegative preservation using bivariate splines and its application, Comput. Aided Geom. Design 34 (2015) 37–49.

[23] V. Baramidze, Smooth bivariate shape-preserving cubic spline approximation, Comput. Aided Geom. Design 44 (2016) 36–55.

[24] A.-R. Diercks, R.C. Highsmith, V.L. Asper, D. Joung, Z. Zhou, L. Guo, A.M. Shiller, S.B. Joye, A.P. Teske, N. Guinasso, et al., Characterization of subsurface polycyclic aromatic hydrocarbons at the deepwater horizon site, Geophys. Res. Lett. 37 (20) (2010).

[25] V. Baramidze, M.J. Lai, Error bounds for minimal energy interpolatory spherical splines, in: Approximation Theory XI: Gatlinburg, Nashboro Press, 2004, pp. 25–50.

[26] V. Baramidze, M.-J. Lai, Convergence of discrete and penalized least squares spherical splines, J. Approx. Theory 163 (9) (2011) 1091–1106.

[27] M.Z. Hussain, M. Hussain, C 1 positivity preserving scattered data interpolation using rational Bernstein-Bézier triangular patch, J. Appl. Math. Comput. 35 (1) (2011) 281–293.

[28] V. Kong, B. Ong, K. Saw, Range restricted interpolation using cubic Bézier triangles, Proc. Comput. Graph. Vis. Comput. Vis. (2004) 125–132.

[29] A.R.M. Piah, T.N. Goodman, K. Unsworth, Positivity-preserving scattered data interpolation, in: Mathematics of Surfaces XI, Springer, 2005, pp. 336–349.

[30] A. Saaban, A. Piah, A. Majid, Performance of the triangulation-based methods of positivity-preserving scattered data interpolation, Far East J. Math. Sci. 57 (1) (2011) 1–11.

[31] M. Sarfraz, M.Z. Hussain, M.A. Ali, Positivity-preserving scattered data interpolation scheme using the side-vertex method, Appl. Math. Comput. 218 (15) (2012) 7898–7910.

[32] M.J. Lai, L.L. Schumaker, Spline Functions on Triangulations, Encyclopedia of Mathematics and Its Applications, Vol. 110, Cambridge University Press, 2007.

[33] M. Neamtu, L.L. Schumaker, On the approximation order of splines on spherical triangulations, Adv. Comput. Math. 21 (1) (2004) 3–20.

[34] Y. Nesterov, Gradient methods for minimizing composite functions, Math. Program. 140 (1) (2013) 125–161.

[35] Y. Nesterov, Introductory lectures on convex optimization, in: A Basic Course, Vol. 87, 2004, p. xviii+ 236.